

Chemical Science

Accepted Manuscript



This is an *Accepted Manuscript*, which has been through the Royal Society of Chemistry peer review process and has been accepted for publication.

Accepted Manuscripts are published online shortly after acceptance, before technical editing, formatting and proof reading. Using this free service, authors can make their results available to the community, in citable form, before we publish the edited article. We will replace this *Accepted Manuscript* with the edited and formatted *Advance Article* as soon as it is available.

You can find more information about *Accepted Manuscripts* in the [Information for Authors](#).

Please note that technical editing may introduce minor changes to the text and/or graphics, which may alter content. The journal's standard [Terms & Conditions](#) and the [Ethical guidelines](#) still apply. In no event shall the Royal Society of Chemistry be held responsible for any errors or omissions in this *Accepted Manuscript* or any consequences arising from the use of any information it contains.



Journal Name

ARTICLE

Directly probing spin dynamics in a molecular magnet with femtosecond time-resolution

J. O. Johansson,^{*a} J.-W. Kim,^b E. Allwright,^a D. M. Rogers,^a N. Robertson^a and J.-Y. Bigot^{*b}

Received 00th January 20xx,
Accepted 00th January 20xx

DOI: 10.1039/x0xx00000x

www.rsc.org/

We show that a vanadium-chromium Prussian Blue analogue, which is a room-temperature molecule-based magnet, displays a fast magnetic response on a femtosecond timescale that is due to the super-exchange interaction between the metal ions. This dynamics is obtained from femtosecond Faraday magneto-optical (MO) measurements, performed at 50 and 300 K. Exciting at the ligand-to-metal charge-transfer (LMCT) band results in the formation of the ²E excited state on the Cr ion via intersystem crossing (ISC) from the ⁴LMCT state in less than 250 fs. Subsequent vibrational relaxation in the ²E state occurs on a 0.78 ± 0.05 ps timescale at 50 K and 1.1 ± 0.1 ps at 300 K. The MO measurements can detect the formation of the ²E state on the Cr ion from the change in the super-exchange interaction taking place as a result of the corresponding spin flip associated with the formation of the ²E state. These studies open up a new avenue to study molecular magnets using a powerful method that is capable of directly probing spin dynamics on a sub-picosecond timescale in thin film environments.

Introduction

The possibility to optically switch the spin configuration of molecular magnets^{1–3} could contribute to the development of applications such as quantum computers, spintronic devices, and high-capacity information-storage devices. Femtosecond laser pulses currently form the only technology able to function beyond one terahertz (10^{12} Hz), allowing for potentially faster switching than the 10–100 gigahertz capabilities of electronic transistors. To study switching processes, a method is needed that is directly sensitive to the spin state and is fast enough to probe on the sub-picosecond timescale relevant for optical excitation. To this end, ultrafast magneto-optical (MO) techniques^{4,5}, such as Faraday rotation, are the only optical methods capable of directly probing spin dynamics on these timescales, as reported in various magnetic metals⁶, dielectrics⁷ and nanoparticles⁸. Applying these techniques to molecular materials therefore offers exciting possibilities since optical spin-manipulation has been achieved in a range of molecule-based magnets^{9–16} and spin-crossover (SCO) systems^{17–29} but so far only x-ray fluorescence using free-electron lasers has provided a direct probe of the sub-ps spin dynamics³⁰.

Faraday rotation is closely related to magnetic circular dichroism (MCD) and occurs due to a difference in index of refraction for left and right circularly polarised light in a

magnetised material³¹. The difference arises because the circular polarisation components interact differently with Zeeman-shifted electronic states whose spin and orbital angular momenta align differently in a magnetic field. Importantly, the Faraday rotation angle is proportional to the sample magnetisation. In time-resolved measurements, the MO signal is obtained by carefully measuring the change in polarisation state of the probe pulse as a function of time delay after exciting the sample with a pump pulse. Ultrafast MO methods have made it possible to untangle spin dynamics from charge and lattice dynamics in ferromagnets after femtosecond laser pulse excitation⁶. They therefore show large potential to distinguish spin and nuclear dynamics in SCO materials, where high-spin and low-spin states are typically distinguished based on changes in optical spectra^{18,23,25,32} and/or bond-lengths^{21,22,24,33–35}, which are not explicitly sensitive to spin dynamics. The power of ultrafast MO Faraday measurements is that they can give details of magnetisation dynamics on the fs timescale.

In this article, we explore the ultrafast MO and transmission dynamics of thin films of the V^{II/III}Cr^{III} Prussian Blue Analogue (PBA), which was chosen as a model system because it is a room-temperature magnet³⁶ with a pronounced static MO response in the visible spectrum^{37,38}. We demonstrate that a change in the spin configuration on the metal ions leads to a sub-picosecond change in the MO signal due to the super-exchange interaction between the metallic ions in the films.

Experimental

Materials

^a EaStCHEM, School of Chemistry, University of Edinburgh, David Brewster Road, EH9 3FJ, UK. Email: olaf.johansson@ed.ac.uk

^b Institut de Physique et Chimie des Matériaux de Strasbourg (IPCMS), UMR 7504, CNRS, Université de Strasbourg, BP 43, 23 rue du Loess, 67034 Strasbourg Cedex 02, France. Email: jean-yves.bigot@ipcms.unistra.fr

The sample and a typical transmittance spectrum are shown in Fig. 1(a). The $V^{II/III}Cr^{III}$ PBA is comprised of Cr ions in their third oxidation state (Cr^{III} , $3d^3$ electrons in the configuration $t_{2g}^3e_g^0$) octahedrally surrounded by cyanide ligands (CN^-) with the carbon end (grey spheres) towards the Cr ions (yellow spheres) and the V ions (green spheres) bound to the nitrogen (blue spheres) end of the ligands (see Fig. 1(b)). In the film, V is present in two different oxidation states, $V^{II}(t_{2g}^3e_g^0)$ and $V^{III}(t_{2g}^2e_g^0)$, and the corresponding ratio is determined by the electrochemical conditions used during deposition³⁷. The electrons are only partially localised on the metal ions and there is some orbital overlap between adjacent ions via the cyanide ligands. This leads to a coupling of the spins via the ligand bridge and the magnetic properties of the PBA

therefore arise from the super-exchange interaction between the metal ions through the cyanide ligand (Fig. 1(b)). Due to the stoichiometry of the materials, vacant sites, and the presence of both V^{II} ($S = 3/2$) and V^{III} ($S = 1$) there is not a complete cancellation of the V spins with respect to the Cr^{III} spins ($S = 3/2$) and consequently the V-Cr PBA is a ferrimagnet.

We electrochemically synthesised thin films of the $V^{II/III}Cr^{III}$ PBA on 3 mm thick fluorine-doped tin oxide (FTO) coated glass substrates under potentiostatic conditions as outlined in refs. ^{37,38}. Aqueous solutions of VCl_3 and $K_3[Cr(CN)_6]$ from Sigma-Aldrich were used without further purification at concentrations of 15 and 10 mM and KCl was used as electrolyte at a concentration of 0.5 M. The substrates were cleaned in an ultrasonic bath using three different solvents (clean substrates were critical in order to produce films of good optical quality and thus reduce the amount of scattered pump light in the time-resolved experiments). A potential of -1.2 V w.r.t. a Pt pseudo-reference electrode was applied for 10 minutes, producing blue-coloured films, which showed transmittance spectra in accordance with literature. Inductively coupled plasma optical emission spectrometry showed a Cr/V ratio of 0.89 and the IR spectrum showed an intense peak at 2106 cm^{-1} assigned to the asymmetric CN^- stretching frequency (SI). The VCr PBAs are air sensitive and so the electrochemistry was performed under N_2 flow. The films were rinsed with N_2 -bubbled H_2O and allowed to dry under N_2 flow. Once dried, they were sealed with cyanoacrylate glue and a 0.18 mm thick glass microscope coverslip.

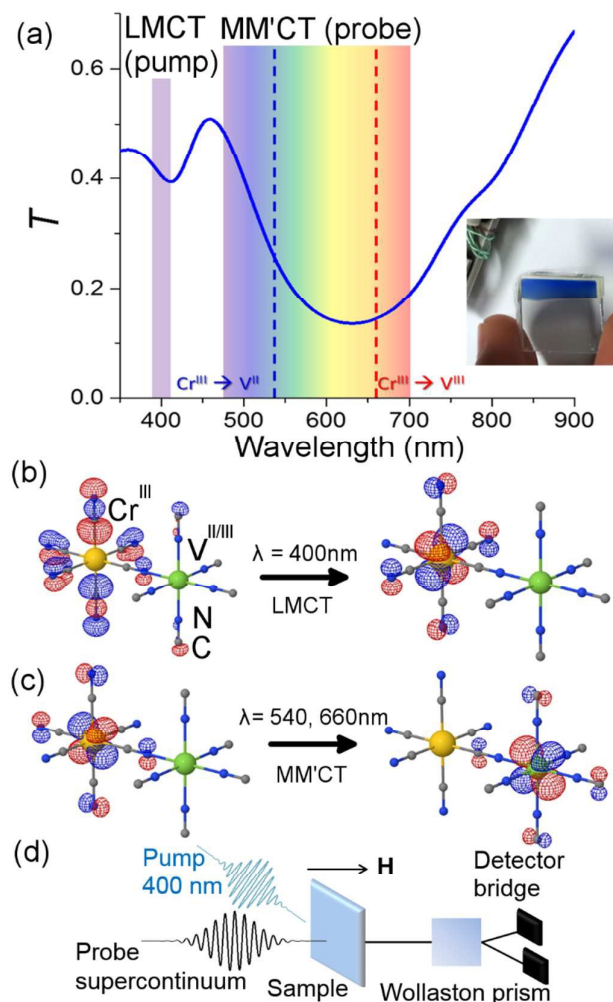


Figure 1: Orbital configuration and transmission associated to the ligand-to-metal and metal-to-metal charge transfer. (a) Static optical transmission spectrum of the film at room temperature. The pump wavelength is assigned to the ligand-to-metal charge transfer (LMCT) transition. The probe wavelengths span the visible part of the spectrum and measure changes related to the metal-to-metal charge-transfer (MM'CT) transitions for the two different V oxidation states present in the material. A photo of the film is shown in the inset. TD-DFT computations show (b) the LMCT transition and (c) the MM'CT transition. (d) Sketch of the femtosecond MO Faraday experimental setup.

Time-resolved configuration

The pump-probe MO configuration is sketched in Fig. 1(d). The laser system is an amplified Titanium Sapphire laser delivering 50 fs pulses at 5 kHz, with a central wavelength at 800 nm. Part of the beam is used to generate the pump pulses by frequency doubling (400 nm) in a β -barium borate crystal. The pump power was adjusted using a combination of a half waveplate and a polariser in order to achieve a pulse energy of 100 nJ. The beam was focused with a 25 cm achromatic lens to achieve a fluence of 0.5 mJ/cm^2 . At this pump energy, the samples were stable for *ca.* 10 min after which some degree of photodegradation was observed. For this reason, all experiments were performed on the same sample but at different sample position for each measurement. The transmittance was checked before and after each measurement and because of the good sample homogeneity it was possible to measure at different spots with the same transmittance. The pump wavelength spectrally overlapped with the ligand-to-metal charge transfer (LMCT) UV bands, where an electron transfers from a CN^- ligand onto the Cr ion (Fig. 1(b)). Another part of the beam is used to generate a supercontinuum ($\lambda = 480 - 690\text{ nm}$) in a Sapphire crystal by self-phase modulation. The supercontinuum is used to measure the time-dependent differential transmission ($\Delta T/T$) and MO response (Faraday rotation, $\Delta\theta_F$). A folded dispersive optical line allows for a partial compensation of the chirp of the probe pulses. A variable slit in this dispersive line allows

selecting narrower spectral probe wavelengths. In total eight wavelength-specific kinetics traces were recorded in the range 480 – 690 nm with 15 nm bandwidth. The fluence in the 15 nm spectral band was ca. a factor 1000 lower than the pump energy. The pump and probe delay line is moved by a stepper motor. The overall pump and probe temporal resolution is ~ 250 fs. The Faraday rotation is measured with a balanced polarisation bridge analysis. The signal-to-noise ratio in the transmission is minimised by an adequate reference signal selected from the incoming probe beam. All signals are detected using a modulation and lock-in synchronous detection scheme^{4,5}. The temperature T_s of the sample is controlled with a cryostat and the magnetic field, applied perpendicular to the sample plane, is provided by a superconducting magnet.

Computational methods

TD-DFT computations were carried out in order to give further support to the assignment of the optical transitions. Due to the complexity of the PBA system, we carried out the calculations for a single monomeric unit comprising: one V with five CN⁻ ligands (with N pointing toward V), one Cr with five CN⁻ ligands (with C pointing toward Cr) and one bridging CN⁻ ligand (with N toward V and C toward V). Gaussian 09³⁹ was employed to perform the TD-DFT calculations using the PBE0 hybrid functional⁴⁰. The calculations were performed at a fixed geometry and the 6-31G(d) basis set⁴¹ was used for V and Cr ions, and the 6-31G(d) basis set^{42,43} for C and N atoms. The symmetry of the monomeric unit was C_{4v} . The calculations for the V^{III}-Cr^{III} PBA showed two transitions with non-zero oscillator strengths in the UV/VIS, namely a LMCT from the CN⁻ ligand to the Cr t_{2g} orbital at 401 nm and a metal-to-metal charge-transfer (MM'CT) transition at 780 nm from the Cr t_{2g} to the V t_{2g} orbitals. For the V^{II}-Cr^{III} PBA system, the transitions were mixed. Here two degenerate LMCT transitions were identified at 324 nm and showed a mix of transfer from the CN⁻ ligand to both Cr and V t_{2g} orbitals. The MM'CT transition was also mixed between transitions between t_{2g} orbitals from Cr to V and V to Cr and occurred at 572 nm. The red-shift of the MM'CT from lower to higher oxidation state of the V (572 and 780 nm, respectively) is in qualitative agreement with experiments³⁷.

Results and discussion

Figure 2 (a) shows $\Delta\theta_F$ at $T_s = 50$ and 300 K for $\lambda = 660$ nm. The signals are recorded for antiparallel magnetic field directions, perpendicular to the sample plane ($H = \pm 0.5$ T), and the difference between the two signals is shown in Fig. 2(b). As is seen in Fig.2(a) – (b), a change in the MO signal occurs on a sub-picosecond timescale. It should be noted that $\Delta\theta_F$ has not been normalised for the static Faraday signal θ_F . The dynamics is fitted with a causal exponential decay, taking into account the Gaussian temporal profile of the pump laser. After a fast rising part, relaxation occurs with time-constants $\tau_{\Delta\theta}$ (50 K) = 0.64 ps and $\tau_{\Delta\theta}$ (300 K) = 1.31 ps at $\lambda=660$ nm. The

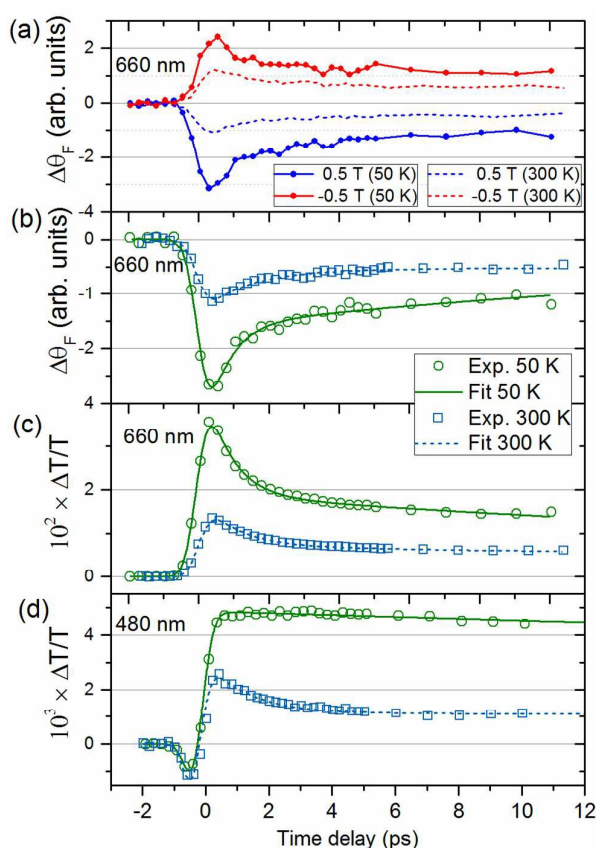


Figure 2: Time-dependent magneto-optical Faraday rotation and transmission of the V-Cr Prussian Blue analogue film. (a) Dynamics of the magneto-optical signals for $H=\pm 0.5$ T, as a function of pump-probe delay for the probe wavelength of $\lambda = 660$ nm at $T_s = 50$ K (solid lines) and 300 K (dashed lines). (b) Fit of the MO Faraday signal and the corresponding transmission dynamics is shown in (c) for $\lambda = 660$ nm. Transmission (d) for $\lambda = 480$ nm for the two temperatures.

corresponding dynamics of the transmission is displayed in Fig. 2(c) with similar time constants $\tau_{\Delta T}$ (50 K) = 0.76 ps and $\tau_{\Delta T}$ (300 K) = 1.05 ps. The fast decay reaches a plateau that slowly decays in several hundreds of picoseconds (shown in SI). For $\lambda=480$ nm (Fig. 2(d)) the dynamics of both $\Delta\theta_F$ and $\Delta T/T$ are different at 50 K, where only the plateau is observed. For this wavelength, a negative signal around zero time delay is also observed at both temperatures.

Figure 3, obtained by interpolation of wavelength-specific kinetic traces, summarises the spectro-temporal dynamics of $\Delta T/T$ and $\Delta\theta_F$ over the whole probe supercontinuum for $T_s = 50$ and 300 K. The maxima of the dynamical spectra are shifted for the two temperatures. The temperature is clearly important for the dynamics after pumping at the LMCT and can be seen to also play a role in the static transmittance spectra of non-photoexcited films (Fig. 3(e)). Figures 3(a) – (d) show that the fast initial decay reaches a plateau (although for $\lambda = 480$ nm at 50 K, the signal immediately reaches the plateau). This is shown in detail in Fig. 2(b) – (c). Figure 3(f) shows the fitted time constants from the wavelength-specific kinetic traces for the decays over the probe spectrum. The decays are faster at $T_s = 50$ K than at 300 K for both $\tau_{\Delta\theta}$ and $\tau_{\Delta T}$.

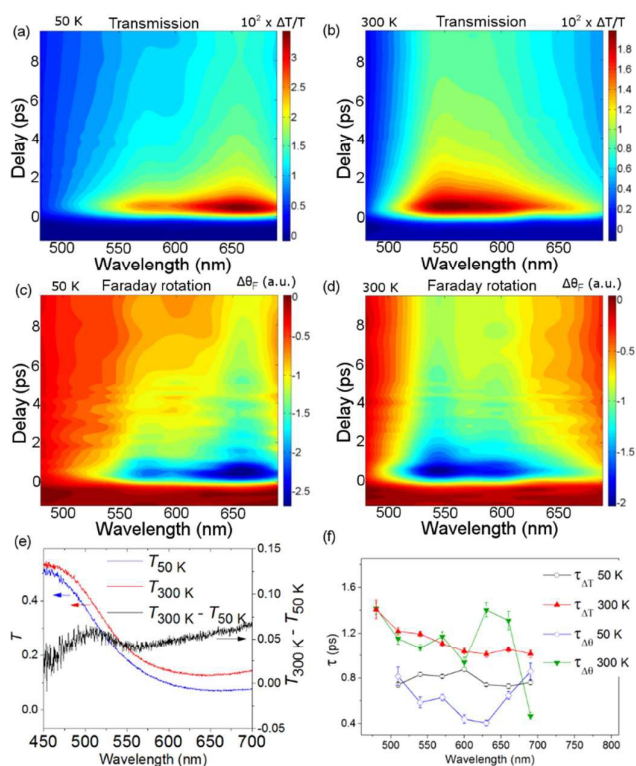


Figure 3: Spectro-temporal dynamics of the transmission and magneto-optical Faraday response for $T_K = 50$ and 300 K. (a) – (b) $\Delta T/T$ and (c) – (d) $\Delta\theta_F$ as a function of wavelength and time delay. (e) Static transmission spectra as a function of temperature. (f) Fitted time constants from the data in (a) – (d).

The overall spin and charge dynamics after the LMCT to Cr are interpreted by considering that the probe pulses overlap with the MM'CT band (Fig. 1(c) and 4(a)). Because of the different oxidation states of the V ions, more energy is required to transfer an electron from a Cr ion to a V^{II} site than to a V^{III} site due to the Coulomb repulsion. This difference results in the splitting of the MM'CT band into two peaks in the transmittance spectrum at 660 nm ($Cr^{III} \rightarrow V^{II}$) and at 540 nm ($Cr^{III} \rightarrow V^{III}$), which is barely seen as a shoulder in the transmittance spectrum shown in Fig. 1(a). Such a peak was observed at 550 nm by Garde *et al.* for $V^{II}Cr^{III}$ PBA molecules in suspension who also assigned it to the MM'CT band⁴⁴. The static Faraday ellipticity spectrum reported by Ohkoshi *et al.*³⁷ gives further support for the two types of charge-transfer. Indeed, in their PBA films the predominance of V^{II} ions strongly reduces the resonance at 660 nm associated to the V^{III} ions.

The increase in transmission of the MM'CT states and subsequent fast decay has to be interpreted by considering that we are pumping at the LMCT transition. In contrast to metallic materials, where the excitation energy is quickly redistributed among all electrons on a femtosecond timescale, the electron dynamics in transition metal complexes depend on the pump wavelength which may excite transitions that are (i) localised ligand-ligand or metal-centred ligand-field (LF) transitions or (ii) partially delocalised LMCT/MLCT or MM'CT transitions. Ultrafast relaxation dynamics after fs excitation in $Cr^{III}(acac)_3$ (acac = deprotonated monoanion of acetylacetonate)

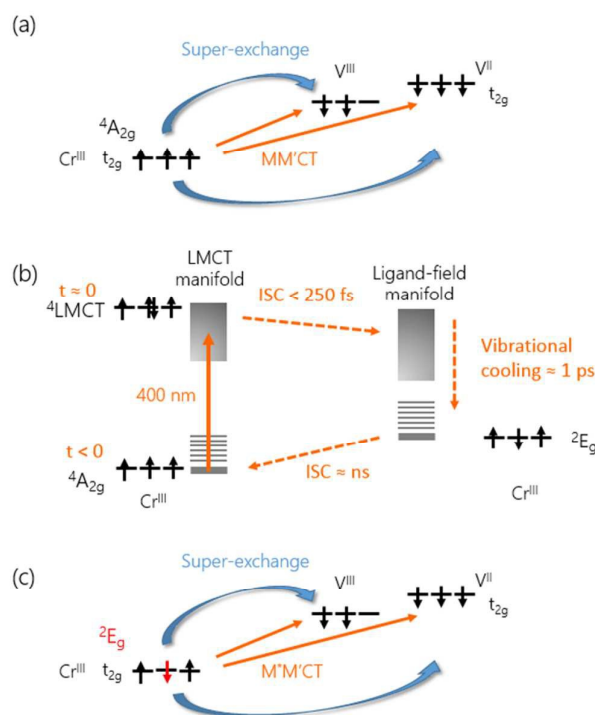


Figure 4: Charge and spin dynamics model. (a) In the ground-state, the MM'CT can occur from the Cr^{III} ions to V^{II} and V^{III} ions. (b) The pump laser excites an electron from a CN⁻ ligand onto the Cr ion (LMCT). The populated 4LMCT state quickly decays to the LF manifold and the vibrationally excited 2E_g state is formed in less than 250 fs. Subsequent vibrational cooling in this state takes place on a ca. 1 ps time scale. The 2E_g state eventually decays back to the ground state via ISC on a ns timescale. The associated change in the super-exchange interaction affects the MO signal of the MM'CT state.

complexes in solution at both LF and LMCT pumping have been extensively studied by Juban and McCusker^{32,45}. They found that the excited 4LMCT state quickly decays via intersystem crossing (ISC) to the 2E_g state of the Cr ion with a 50 fs time constant. Subsequent decay kinetics of the signal on a 1.1 ps timescale was attributed to vibrational cooling in the 2E_g . The 2E_g state eventually decays back via ISC to the 4A_2 ground state on a ns timescale. ISC on timescales shorter than 100 fs after LMCT excitation is known to occur in Fe^{II} SCO complexes in solution²³ and it has been reported that similar dynamics, localised on the Fe sites in the lattice, can be observed in SCO crystals^{21,25}. It is therefore plausible that the decay processes described by Juban and McCusker^{32,45} are applicable to the dynamics of the Cr ions in the $V^{II/III}Cr^{III}$ PBA lattice. It should be noted that for the shortest wavelength ($\lambda = 480$ nm, Fig. 2(d)) we observe a very fast transient decrease of the transmission, which we attribute to an excited-state absorption (ESA) from the 4LMCT state. The subsequent fast decay of the ESA at 480 nm (180 ± 30 fs at 50 K and 110 ± 10 fs at 300 K, both time constants shorter than the experimental time resolution), which occurs at the very beginning of the pump-probe $\Delta T/T$ signal, further supports the short life-time of the 4LMCT state. The subsequent formation of the excited 2E_g state corresponds to a spin flip of one of the electrons in a t_{2g} orbital and for this

reason we will hereafter name the metal-to-metal charge-transfer process $M^*M'CT$ instead of $MM'CT$, where M^* indicates an excited state of the Cr ion. The new spin configuration on the Cr site will affect the $M^*M'CT$ transition leading to a reduction in the $MM'CT$ absorption causing the increase in the transmission that we observe experimentally. The vibrational cooling in the 2E state is responsible for the ~ 0.8 ps at 50 K and ~ 1.1 ps at 300 K decay kinetics of the transient transmission that we observe (Fig. 4(b)). We do not observe any ESA from the 2E state⁴⁵, presumably because changes to the visible spectrum is completely dominated by the much stronger $M^*M'CT$ transition.

The propensity to optically transfer to either V^{II} or V^{III} from the excited-state potential, and the corresponding timescale for which this occurs, depends on the sample temperature, as observed in Fig. 3(a), (b) and (f). The temperature dependence of the $M^*M'CT$ absorption band should therefore be different from the temperature dependence of the ground-state $MM'CT$ band as displayed in the static spectrum of Fig. 3(e). The above interpretation of a temperature-dependent decay pathway after the LMCT excitation is further sustained by the results of Bozdogan *et al.*⁴⁶ who identified a hidden metastable state that caused a decrease in the magnetisation after illuminating a sample of V-Cr PBA for 60 h at the LMCT transition at 10 K ($\lambda = 350$ nm). In their results, the metastable state survives heating up to 250 K and disappears at higher temperatures indicating the efficient role played by thermal excitations in PBAs.

Let us now focus on the differential magneto-optical Faraday signal $\Delta\theta_F$ measured at temperatures $T_s = 50$ and 300 K. Electronic optical transitions that affect exchange-coupled electrons give rise to a MO signal whose magnitude and sign depend on the nature of the transition³¹. Ohkoshi *et al.* have shown that the MO signal from the $MM'CT$ transition in VCr PBA is proportional to the magnetisation³⁷. This arises because the spins on the Cr ions are connected to the spins on the V ions via the super-exchange interaction. In contrast, there is no static MO signal from the LMCT transition³⁷, which is probably due to the fully occupied orbital of the ligand and so there is no exchange interaction between the electrons on the ligand and the Cr ion. In our experiments, we observe similar decay constants as for $\Delta T/T$, which is shown in Fig. 3(f). After the fast ISC to the 2E state on the Cr ion, the new spin configuration is changed from $S = 3/2$ to $S = 1$ (Fig. 4(c)). The local change in spin configuration modifies the super-exchange interaction between the Cr and V ions and therefore gives rise to the change in MO signal of the $M^*M'CT$ transition. The time-resolved MO can therefore detect changes to the strength of the super-exchange interaction on a sub-ps timescale.

Besides from the large range of studies on SCO compounds mentioned previously, where fast ISC occurs accompanied by structural changes, other molecular magnetic systems also display fast dynamics. For example, fast sub-50 fs three-state dynamics, involving partly spin-allowed steps, have been observed in breathing crystals using transient absorption¹². In Prussian Blue, both ultrafast back-electron transfer and trapping of charge-transfer (CT) states occur after exciting at the $MM'CT$ transition^{47,48}. This has also been observed in

related dinuclear cyano-bridged mixed-valence systems⁴⁹. Trapping of long-lived CT states (ns) in the photomagnetic $Co^{II}Fe^{III}$ PBA was also observed after both $MM'CT$ and LMCT pumping⁵⁰.

Conclusions

In conclusion, we have observed the ultrafast dynamics of charge and spin transfer in the molecule-based magnet V-Cr PBA at room temperature and 50 K. It has been carried out by performing time-resolved femtosecond transmission and magneto-optical Faraday measurements with frequency non-degenerate pumping (400 nm) and probing (super-continuum in the visible). We show that upon exciting the ligand-to-metal charge-transfer transition at 400 nm, the 2E states on the Cr sites are populated in less than 250 fs, resulting in an increase in the transmission associated with the $M^*M'CT$ transition. Vibrational cooling in the 2E state occurs with a time constant of 0.78 ± 0.05 ps at 50 K and 1.1 ± 0.1 ps at 300 K. Correspondingly the time-dependent MO Faraday signal follows the same dynamics and the associated change in spin-configuration of the 2E state is observable in the MO signal of the $M^*M'CT$ transition. The results show that the method can be used to directly observe changes to spin configurations, and therefore the exchange interaction, on fs timescales in magnetic molecular materials. The signature from both V oxidation states implies that the present approach of studying site-specific dynamics using ultrafast laser spectroscopy together with time-resolved magneto-optics is a powerful and underexplored technique for the field of molecular magnetism, especially when selective pumping and broad-band spectral probing are employed. This in turn will allow for new chemistry to be developed in the process of optimising magneto-optical properties and spin switching rates by chemically tuning the molecular properties. A sudden change in spin configuration can lead to a large structural change, as in the case of spin-crossover materials, which typically leads to vibrational dynamics such as stretching and bending modes^{21,23,25}. The proposed method here is fast enough to follow the vibrational dynamics of magneto-structural correlations by simultaneously recording the transmission and MO signals. Faraday MO can therefore provide an attractive alternative approach to directly probe the spin dynamics in molecule-based magnets, single-molecule magnets, and spin-crossover materials. These studies show the large potential of femtomagnetism for studying and monitoring molecular magnets.

Acknowledgements

The authors thank the European Research Council for financial support via the Advanced Grant project "ATOMAG" ERC-2009-AdG-20090325 #247452. JOJ acknowledges financial support from the Royal Society of Edinburgh and fruitful discussions with E. Brechin. JOJ is a Royal Society of Edinburgh/BP Trust Research Fellow.

References

- 1 D. Gatteschi, R. Sessoli and F. Villain, *Molecular Nanomagnets*, Oxford Univ. Press, New York, 2007.
- 2 G. Christou, D. Gatteschi, D. N. Hendrickson and R. Sessoli, *MRS Bull.*, 2011, **25**, 66–71.
- 3 J. S. Miller, *Chem. Soc. Rev.*, 2011, **40**, 3266–3296.
- 4 J.-Y. Bigot and M. Vomer, *Ann. Phys.*, 2013, **525**, 2–30.
- 5 A. Kirilyuk, A. V. Kimel and T. Rasing, *Rep. Prog. Phys.*, 2013, **76**, 026501.
- 6 E. Beaurepaire, J.-C. Merle, A. Daunois and J.-Y. Bigot, *Phys. Rev. Lett.*, 1996, **76**, 4250–4253.
- 7 A. V. Kimel, A. Kirilyuk, P. A. Usachev, R. V. Pisarev, A. M. Balbashov and T. Rasing, *Nature*, 2005, **435**, 655–657.
- 8 J.-Y. Bigot, H. Kesserwan, V. Halté, O. Ersen, M. S. Moldovan, T. H. Kim, J. T. Jang and J. Cheon, *Nano Lett.*, 2012, **12**, 1189–1197.
- 9 O. Sato, T. Iyoda, A. Fujishima and K. Hashimoto, *Science*, 1996, **272**, 704–705.
- 10 S. Ohkoshi and H. Tokoro, *Acc. Chem. Res.*, 2012, **45**, 1749–1758.
- 11 D. Pejaković, C. Kitamura, J. S. Miller and A. J. Epstein, *Phys. Rev. Lett.*, 2002, **88**, 057202.
- 12 W. Kaszub, A. Marino, M. Lorenc, E. Collet, E. G. Bagryanskaya, E. V. Tretyakov, V. I. Ovcharenko and M. V. Fedin, *Angew. Chemie Int. Ed.*, 2014, **53**, 10636–10640.
- 13 D. M. Pajerowski, M. J. Andrus, J. E. Gardner, E. S. Knowles, M. W. Meisel and D. R. Talham, *J. Am. Chem. Soc.*, 2010, **132**, 4058–4059.
- 14 O. N. Risset, T. V. Brinzari, M. W. Meisel and D. R. Talham, *Chem. Mater.*, 2015, **27**, 6185–6188.
- 15 S. Ohkoshi, K. Imoto, Y. Tsunobuchi, S. Takano and H. Tokoro, *Nat. Chem.*, 2011, **3**, 564–569.
- 16 D. Aguilà, Y. Prado, E. S. Koumoussi, C. Mathonière and R. Clérac, *Chem. Soc. Rev.*, 2016, **45**, 203–224.
- 17 A. Bousseksou, G. Molnár, L. Salmon and W. Nicolazzi, *Chem. Soc. Rev.*, 2011, **40**, 3313–3335.
- 18 A. Marino, M. Servol, R. Bertoni, M. Lorenc, C. Mauriac, J. F. Létard and E. Collet, *Polyhedron*, 2013, **66**, 123–128.
- 19 A. Cannizzo, C. J. Milne, C. Consani, W. Gawelda, C. Bressler, F. van Mourik and M. Chergui, *Coord. Chem. Rev.*, 2010, **254**, 2677–2686.
- 20 R. Bertoni, M. Lorenc, H. Cailleau, A. Tissot, J. Laisney, M.-L. Boillot, L. Stoleriu, A. Stancu, C. Enachescu and E. Collet, *Nat. Mater.*, 2016, **15**, 606–610.
- 21 M. Cammarata, R. Bertoni, M. Lorenc, H. Cailleau, S. Di Matteo, C. Mauriac, S. F. Matar, H. Lemke, M. Chollet, S. Ravy, C. Laulhé, J.-F. Létard and E. Collet, *Phys. Rev. Lett.*, 2014, **113**, 227402.
- 22 S. E. Canton, X. Zhang, L. M. Lawson Daku, A. L. Smeigh, J. Zhang, Y. Liu, C. Wallentin, K. Attenkofer, G. Jennings, C. A. Kurtz, D. Gosztola, K. Wärnmark, A. Hauser and V. Sundström, *J. Phys. Chem. C*, 2014, **118**, 4536–4545.
- 23 G. Auböck and M. Chergui, *Nat. Chem.*, 2015, **7**, 629–633.
- 24 C. Bressler, C. Milne, V.-T. Pham, A. ElNahas, R. M. van der Veen, W. Gawelda, S. Johnson, P. Beaud, D. Grolimund, M. Kaiser, C. N. Borca, G. Ingold, R. Abela and M. Chergui, *Science (80-)*, 2009, **323**, 489–492.
- 25 R. Field, L. C. Liu, W. Gawelda, C. Lu and R. J. D. Miller, *Chem. - A Eur. J.*, 2016, **22**, 5118–5122.
- 26 A. Hauser and C. Reber, in *Structure and Bonding*, Springer Berlin Heidelberg, 2016, vol. 119, pp. 193–223.
- 27 M. Halcrow, *Spin-Crossover Materials: Properties and Applications*, Wiley VCH, 2013.
- 28 P. Gütllich, A. Hauser and H. Spiering, *Angew. Chemie Int. Ed. English*, 1994, **33**, 2024–2054.
- 29 A. Hauser, in *TOPICS IN CURRENT CHEMISTRY*, eds. P. Gütllich and H. A. Goodwin, Springer, Heidelberg, 2004, pp. 155–198.
- 30 W. Zhang, R. Alonso-Mori, U. Bergmann, C. Bressler, M. Chollet, A. Galler, W. Gawelda, R. G. Hadt, R. W. Hartscock, T. Kroll, K. S. Kjær, K. Kubiček, H. T. Lemke, H. W. Liang, D. a. Meyer, M. M. Nielsen, C. Purser, J. S. Robinson, E. I. Solomon, Z. Sun, D. Sokaras, T. B. van Driel, G. Vankó, T.-C. Weng, D. Zhu and K. J. Gaffney, *Nature*, 2014, **509**, 345–348.
- 31 K. Shinagawa, in *Magneto-Optics*, eds. S. Sugano and N. Kojima, Springer-Verlag, Berlin, 2000, pp. 137–178.
- 32 E. A. Juban, A. L. Smeigh, J. E. Monat and J. K. McCusker, *Coord. Chem. Rev.*, 2006, **250**, 1783–1791.
- 33 G. Vankó, P. Glatzel, V.-T. Pham, R. Abela, D. Grolimund, C. N. Borca, S. L. Johnson, C. J. Milne and C. Bressler, *Angew. Chemie Int. Ed.*, 2010, **49**, 5910–5912.
- 34 A. L. Smeigh, M. Creelman, R. a. Mathies and J. K. McCusker, *J. Am. Chem. Soc.*, 2008, **130**, 14105–14107.
- 35 N. Huse, H. Cho, K. Hong, L. Jamula, F. M. F. de Groot, T. K. Kim, J. K. McCusker and R. W. Schoenlein, *J. Phys. Chem. Lett.*, 2011, **2**, 880–884.
- 36 S. Ferlay, T. Mallah, R. Ouahès, P. Veillet and M. Verdaguer, *Nature*, 1995, **378**, 701–703.
- 37 S. Ohkoshi, M. Mizuno, G. Hung and K. Hashimoto, *J. Phys. Chem. B*, 2000, **104**, 9365–9367.
- 38 M. Verdaguer, M. Glavez, R. Garde and C. Desplanches, *Electrochem. Soc. Interface*, 2002, **11**, 28.
- 39 M. J. Frisch, G. W. Trucks, H. B. Schlegel, G. E. Scuseria, M. A. Robb, J. R. Cheeseman, G. Scalmani, V. Barone, B. Mennucci, G. A. Petersson, H. Nakatsuji, M. Caricato, X. Li, H. P. Hratchian, A. F. Izmaylov, J. Bloino, G. Zheng, J. L. Sonnenberg, M. Hada, M. Ehara, K. Toyota, R. Fukuda, J. Hasegawa, M. Ishida, T. Nakajima, Y. Honda, O. Kitao, H. Nakai, T. Vreven, J. A. Montgomery Jr., J. E. Peralta, F. Ogliaro, M. Bearpark, J. J. Heyd, E. Brothers, K. N. Kudin, V. N. Staroverov, R. Kobayashi, J. Normand, K. Raghavachari, A. Rendell, J. C. Burant, S. S. Iyengar, J. Tomasi, M. Cossi, N. Rega, J. M. Millam, M. Klene, J. E. Knox, J. B. Cross, V. Bakken, C. Adamo, J. Jaramillo, R. Gomperts, R. E. Stratmann, O. Yazyev, A. J. Austin, R. Cammi, C. Pomelli, J. W. Ochterski, R. L. Martin, K. Morokuma, V. G. Zakrzewski, G. A. Voth, P. Salvador, J. J. Dannenberg, S. Dapprich, A. D. Daniels, Ö. Farkas, J. B. Foresman, J. V. Ortiz, J. Cioslowski and D. J. Fox, *Gaussian Inc Wallingford CT*, 2009, 34, Wallingford CT.
- 40 C. Adamo and V. Barone, *J. Chem. Phys.*, 1999, **110**, 6158.
- 41 A. J. H. Wachters, *J. Chem. Phys.*, 1970, **52**, 1033.

- 42 P. C. Hariharan and J. a. Pople, *Theor. Chim. Acta*, 1973, **28**, 213–222.
- 43 W. J. Hehre, R. Ditchfield and J. A. Pople, *J. Chem. Phys.*, 1972, **56**, 2257–2261.
- 44 R. Garde, F. Villain and M. Verdaguer, *J. Am. Chem. Soc.*, 2002, **124**, 10531–10538.
- 45 E. A. Juban and J. K. McCusker, *J. Am. Chem. Soc.*, 2005, **127**, 6857–6865.
- 46 K. D. Bozdog, J.-W. Yoo, N. P. Raju, A. C. McConnell, J. S. Miller and A. J. Epstein, *Phys. Rev. B*, 2010, **82**, 094449.
- 47 D. C. Arnett, P. Voehringer and N. F. Scherer, *J. Am. Chem. Soc.*, 1995, **117**, 12262–12272.
- 48 D. Weidinger, D. J. Brown and J. C. Owrutsky, *J. Chem. Phys.*, 2011, **134**, 124510.
- 49 B. P. Macpherson, P. V Bernhardt, A. Hauser, S. Pagès and E. Vauthey, *Inorg. Chem.*, 2005, **44**, 5530–5536.
- 50 H. Kamioka, Y. Moritomo, W. Kosaka and S. Ohkoshi, *Phys. Rev. B*, 2008, **77**, 180301.